

Fiber optic monitoring methods for composite steel-concrete structures based on determination of neutral axis and deformed shape

FINAL REPORT

January 2014

Submitted by:

Branko Glisic

Assistant Professor

Princeton University

Princeton University E330 EQuad

Princeton, NJ 08544

Submitted to:

New Jersey Department of Transportation

Dave Lambert

Nagnath Kasbekar

In cooperation with

Rutgers, The State University of New Jersey

And

New Jersey Department of Transportation

And

U.S. Department of Transportation

Federal Highway Administration

Disclaimer Statement

The contents of this report reflect the views of the authors, who are responsible for the facts and the accuracy of the information presented herein. This document is disseminated under the sponsorship of the Department of Transportation, University Transportation Centers Program, in the interest of information exchange. The U.S. Government assumes no liability for the contents or use thereof.

The Center for Advanced Infrastructure and Transportation (CAIT) is a Tier I UTC Consortium led by Rutgers, The State University. Members of the consortium are the University of Delaware, Utah State University, Columbia University, New Jersey Institute of Technology, Princeton University, University of Texas at El Paso, University of Virginia and Virginia Polytechnic Institute. The Center is funded by the U.S. Department of Transportation.

1. Report No. CAIT-UTC-012	2. Government Accession No.	3. Recipient's Catalog No.	
4. Title and Subtitle Fiber optic monitoring methods for composite steel-concrete structures based on determination of neutral axis and deformed shape		5. Report Date January 2014	
		6. Performing Organization Code CAIT/Princeton University	
7. Author(s) Branko Glisic		8. Performing Organization Report No. CAIT-UTC-012	
9. Performing Organization Name and Address Princeton University E330 EQuad Princeton, NJ 08544		10. Work Unit No.	
		11. Contract or Grant No. DTRT12-G-UTC16	
12. Sponsoring Agency Name and Address Center for Advanced Infrastructure and Transportation Rutgers, The State University of New Jersey 100 Brett Road Piscataway, NJ 08854		13. Type of Report and Period Covered Final Report 06/15/2012 – 11/30/2013	
		14. Sponsoring Agency Code	
15. Supplementary Notes U.S. Department of Transportation/Research and Innovative Technology Administration 1200 New Jersey Avenue, SE Washington, DC 20590-0001			
16. Abstract <p>Structural Health Monitoring has great potential to provide valuable information about the actual structural condition and can help optimize the management activities. However, few effective and robust monitoring methods exist which hinders a nationwide use of SHM in structural condition evaluations. The objective of this project was to research and develop methods for structural identification and damage detection based on strain monitoring using long-gauge fiber-optic sensors. In particular two universal parameters of beam-like structures were studied in detail: the neutral axis and deformed shape. Data from two structures were used for validation purposes: from on-site monitoring of the US202/NJ23 overpass and from lab testing of a scale-model of a similar structure. The conclusions are that while the neutral axis varies during dynamic events, it changes the location due to damage, and it can be located accurately using a probabilistic approach. Thus, it can be used as a damage sensitive feature. At least two sensors per cross-section are necessary for an accurate evaluation of the location of the neutral axis. The vertical displacement of beams can be calculated by double integration of the curvature. However, the double integration method affects the accuracy of the evaluation, and to achieve the most accurate result a linear combination of integration methods is recommended. At least three locations along each girder should be instrumented with two parallel sensors for accurate evaluation of the vertical displacement. The methodologies researched in this project are presented in this report and recommendations for the use of the methods provided.</p>			
17. Key Words Fiber optic sensors, Structural health monitoring methods, composite steel-concrete structures, neutral axis, deformed shape		18. Distribution Statement	
19. Security Classification (of this report) Unclassified	20. Security Classification (of this page) Unclassified	21. No. of Pages 20	22. Price

Acknowledgments

Structural health monitoring project on the US202/NJ23 highway overpass in Wayne, realized within the International Bridge Study (IBS), and the ANDERS project were instrumental for this project. These projects have been realized with important support, great help, and kind collaboration from several professionals and companies. We would like to thank: SMARTEC SA, Switzerland; Drexel University, in particular Professor Emin Aktan, Professor Frank Moon, and graduate student Jeff Weidner; New Jersey Department of Transportation (NJDOT); Long-Term Bridge Performance (LTBP) Program of Federal Highway Administration; PB Americas, Inc., Lawrenceville, NJ, in particular Mr. Michael S. Morales, LTBP Site Coordinator; Rutgers University, in particular Professors Ali Maher and Nenad Gucunski as well as members of Professor Gucunski's research group: Seong-Hoon Kee and Matthew Klein; Jersey Precast Inc., in particular Ross Jamieson; All IBS partners; Kevin, the lift operator, Phil, the truck driver, and Joe Vocaturo for technical support; Ed Wass lab manager; Students: Yao Yao, Hiba Abdel-Jaber, Michael Roussell, Kaitlyn Kliewer, Tiffany Hwang, and Katherine Flanigan for helping with sensor installation and data acquisition.

Table of Contents	Page
DESCRIPTION OF THE PROBLEM	1
APPROACH	2
METHODOLOGY	2
FINDINGS	4
CONCLUSIONS	12
RECOMMENDATIONS	13
REFERENCES	14

List of Figures

Figure 1. Span 2 of US202/NJ23: a) North and southbound. b) Supports at south end of southbound span.	2
Figure 2. a) Strain diagram over the height of the cross-section during one event from strain measurements at the top and bottom sensor taken at 250Hz. b) Histogram from approximately 60 events. The mean is close to the theoretical location of the neutral axis. If there is delamination in the cross-section the neutral axis location will move.	3
Figure 3. a) Curvature distributions due to passage of a truck; b) deformed shapes calculated by double integration of curvatures using trapezoidal rule.	4
Figure 4. Long-term monitoring of the neutral axis location. The mean for each measurement session along with one standard deviation. This cross-section shows healthy behavior with the mean close to the theoretical location of the neutral axis.	5
Figure 5. Numerical model of the study span of US202/NJ23 and the simulated load pattern.	5
Figure 6. Dynamic event: total strain at location 5.1, 5.2, and 5.3 under the real event and simulated event.	6
Figure 7. Strain diagram from numerical model. a) Dead load applied to the structure, the neutral axis is constant. b) Dynamic event applied to the structure, the neutral axis varies.	6
Figure 8. Cross-section of the test structure. Three steel girders supporting a concrete slab. Four strain sensors are installed in three cross-sections. Location A has delamination, location F is healthy, and location K has a crack.	7
Figure 9. Test structure. The artificial damage is created by placing plastic sheets in the concrete. The sensors are surface mounted on the steel flanges and embedded in the concrete.	7
Figure 10. Test structure with test load. The photo is taken during static testing.	8
Figure 11. Studying the dataset for concrete and steel sensors separately and all four sensors together. On the left, a potential scenario is illustrated where studying different combination leads to different conclusions. On the right the histograms for the healthy location.	8

Figure 12. Delamination is created by placing a plastic sheet horizontally in the concrete. Photos show the sheet and the sensor installed next to it. The histogram is from the measurements of the steel mounted sensors from the delaminated cross-section.	9
Figure 13. The crack is created by placing a plastic sheet vertically in the concrete. Photos show the sheet and the sensor installed next to it. The histogram is from the measurements of the steel mounted sensors from the cracked cross-section.	9
Figure 14. Static test. The truck applies two point loads to the structure. The corresponding curvature diagram is shown. The solid line represents the linear theory of beams and the dashed line corresponds to the measured value at midspan. The three integration rules: Trapezoidal, Rectangular I, and Rectangular II are shown below.	10
Figure 15. Displacements calculated by double integration using the Trapezoidal rule, Rectangular rule I, and Rectangular rule II for three sensor combinations, concrete, steel, and all. The LVDT measurements lie between the two estimations.	11
Figure 16. Displacement at midspan, using steel sensors at location F. The results from the three double integration methods are shown, the combination of the Trapezoidal and Rectangular II, as well as the measurements from the LVDTs. The photo shows LVDTs as installed at center span during static testing.	12

List of Tables

Table 1. Summary of the results from dynamic testing for the three locations, A, F, and K using the three different sensor groups: in concrete, on steel, and all four sensors.	9
Table 2. The ratio: curvature/displacement according to beam theory, the LVDT measurements, and the three integration rules.	12

DESCRIPTION OF THE PROBLEM

The U.S. civil infrastructure is aging and has been identified as an area in critical need of improvement and renovation by several institutions, including the Federal Highway Administration (USDOT, FHWA 2007), the Transportation Research Board (TRB 2007), and the National Institute of Standards and Technology (NIST 2009). In 2011, approximately 24% of U.S. bridges were identified as structurally deficient or functionally obsolete (USDOT, FHWA 2013a). The ratings of bridges are evaluated after regular inspections (mostly visual) according to regulations (U.S. National Archives 2004). Nevertheless, inaccessibility and the large size of bridges can make visual inspection very challenging, and the outcome of the inspection inaccurate and/or incomplete. This is confirmed by numerous unscheduled bridge closures, replacements, and sometimes by catastrophic events (the I-35W Minneapolis Bridge is a recent example (MnDOT 2009)). Structural Health Monitoring (SHM) has great potential to provide valuable information about the actual structural condition and can aid in early detection and evaluation of damage and deterioration that are invisible to the human eye. However, few effective and robust monitoring and data analysis techniques exist which hinders a nationwide use of SHM in structural condition evaluations.

Bridges are essential links which connect regions across major obstacles. The most common bridge systems in the U.S. are composed of beams; in fact, 60% of the U.S. bridge network is composed of beam systems such as multi-, T-, box-, and channel- beams (USDOT, FHWA 2013b). These typical bridges account for 70% of all deficient bridges in the U.S. (USDOT, FHWA 2013a & 2013b). Insights into true structural behavior, capacity, and vulnerability of this bridge type are a necessity for efficient, effective, and economical preservation actions. Therefore, creating monitoring and analysis methods using parameters which are universal for all beam-like structures will have potential wide applicability for existing and new infrastructure.

The objective of this project was to research and develop methods for structural identification and damage detection based on strain monitoring using long-gauge fiber-optic sensors. In particular two parameters were studied in detail. 1) The location of the neutral axis based on dynamic strain measurements and probabilistic data analysis, and 2) the deformed shape of individual girders based on static strain measurements. Information about these parameters on a local level at several locations was used to perform global structural identification including overall girder and slab interaction. Changes in the neutral axis and deformed shape when monitored over time can indicate change in structural behavior due to damage. The proposed methods do not require testing of the structure, as the data from in-service traffic loading will be used. This is a large advantage as no road-closures are necessary. The neutral axis and deformed shape are universal parameters, and they can be evaluated for any load-carrying beam structure. The methods developed in this project will therefore be applicable to a variety of typical structures. Furthermore this research focused on developing robust data analysis algorithms based on a limited number of sensors. In summary, the methodology is based on simple deployment of the monitoring system, no interruptions of the flow of traffic, reliable analysis algorithms, and it is applicable to a large variety of structures. This project is the first step towards attaining this objective; the results and findings will be used to guide future research of the methodology.

APPROACH

This research has two parts; on-site monitoring of the US202/NJ23 overpass and lab testing of a scale-model of a similar structure. A monitoring system was in place and functioning on the US202/NJ23 through the LTBP program. The scale-model was constructed with artificial damage within the ANDERS project led by Rutgers University. As part of this research, long-gauge fiber-optic sensors were installed at artificially damaged and undamaged locations. Lab tests allow for embedment of sensors in the concrete in addition to steel surface installation, providing information about the slab and girder interaction unattainable (with the current monitoring system) from the real structure. Dynamic and static testing of the model was performed. The test data is compared to the full-scale data.

METHODOLOGY

The methodology is based on long-gauge fiber optic strain and temperature sensors installed in parallel topology. On the real structure (US202/NJ23) the sensors are 1 or 2 m long (depending on the location) installed on the upper and lower flange of the steel girders, see Figures 1 and 2. Three sensor locations are studied in this research; two quarter-span and one midspan location of the center girder (Girder No. 5). The data was collected at 250Hz during the passage of large vehicles over the bridge. No interruption of traffic was needed in order to collect the data, further emphasizing the importance to create methods that can be non-intrusive and widely applicable.

On the scale-model the sensor configuration was similar to the real structure: long-gauge sensors (0.5 m) were installed (within the scope of this project) in a parallel topology. Since the sensors were installed during construction it was possible to embed sensors in the concrete.



Figure 1. Span 2 of US202/NJ23: a) North and southbound. b) Supports at south end of southbound span.

Two parameters, the neutral axis and the deformed shape, were studied in this project. Following is a brief overview of the methodology as it pertains to each parameter.

The neutral axis is a set of points (curve) in a cross-section of a beam at which normal stress and strain vanishes under given loads. The centroid of stiffness (or centroid) is the geometric center (point) weighted with the material stiffness in every point. The centroid is a geometric and material property and its position is theoretically constant for a given, undamaged cross-section. The position of the neutral axis, however, depends on the loading. The centroid is a universal parameter of cross-sections of every load-carrying beam. A change in the position of the centroid within a given cross-section indicates unusual structural behaviors. Since the positions of the neutral axis and the centroid are correlated, a change in position of the centroid affects the position of the neutral axis.

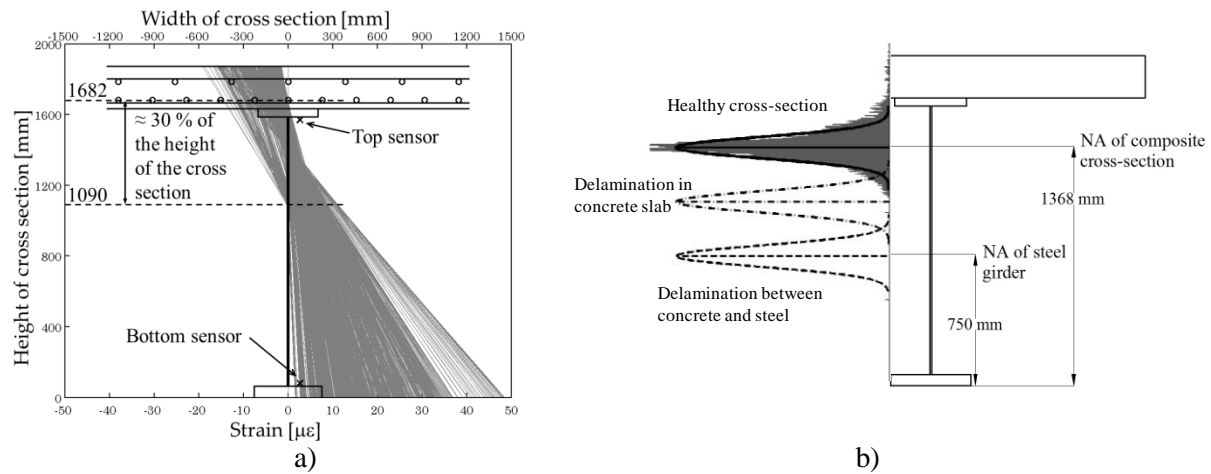


Figure 2. a) Strain diagram over the height of the cross-section during one event from strain measurements at the top and bottom sensor taken at 250Hz. b) Histogram from approximately 60 events. The mean is close to the theoretical location of the neutral axis. If there is delamination in the cross-section the neutral axis location will move.

To be able to use the position of the neutral axis as a damage sensitive feature it is necessary to identify and estimate uncertainties associated with its localization, so the undamaged and damaged states can be characterized and discrimination thresholds can be set. Figure 2a shows the strain diagram during one event (strain measured at 250Hz). The figure shows that during one event the neutral axis varies significantly over the height of the cross-section. This makes a deterministic approach of localization of the neutral axis extremely challenging. A methodology has been developed to accurately locate the neutral axis (Sigurdardottir & Glisic 2013). The essence of this method is depicted in Figure 2b. The neutral axis is evaluated for several events during each measurement session and the histogram of the evaluations is shown in Figure 2b. The histogram reflects a Gaussian distribution the mean of which provides an excellent estimation of the location of the neutral axis. The hypothesis is that if the steel girder and concrete slab become disconnected or delaminated the neutral axis location will move towards a new mean. Note that the results presented in the figure are collected on a real bridge under traffic loading, i.e., with no testing or closure of the bridge.

The deformed shape is a consequence of straining the structure and it is defined by the centroid line of the beam after the deformation. It is well known that the curvature distribution in a deformed beam equals the second derivative of the deformed shape. Thus, any unusual change in global structural behavior that affects the strain (and curvature) also affects the deformed shape. Assuming linearity and the validity of Bernoulli's hypothesis uniaxial curvature can be determined from two strain measurements (e.g. as the slope of the strain diagram presented in Figure 2a).

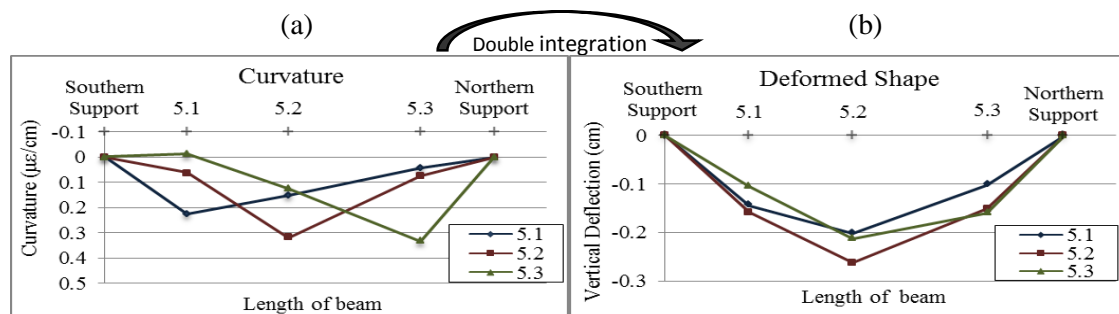


Figure 3. a) Curvature distributions due to passage of a truck; b) deformed shapes calculated by double integration of curvatures using trapezoidal rule.

In this project the double integration is performed using a weighted combination of classical Newton–Cotes formulae. The formulae can be chosen based on loads, so they minimize the uncertainties in double integration for this given load. An example of preliminary results, a set of deformed shapes obtained by double integration of curvature using trapezoidal rule is given in Figure 3. Data is collected on the US202/NJ23 overpass in Wayne, NJ under the passage of a heavy truck, and the graphs represent the deformed shapes when the truck was at locations 5.1, 5.2, and 5.3 (sensors are at the same locations).

FINDINGS

Variability of position of the neutral axis under dynamic loads

The US202/NJ23 highway overpass located near Wayne in New Jersey represents a typical structure frequently found across The United States, see Figure 1. It was built in 1984 and is now part of the Long Term Bridge Performance (LTBP) Program put forth by the Federal Highway Administration. North and southbound traffic is carried by two separate structures; each structure is comprised of four simply supported spans, with eight steel girders carrying a concrete slab. The focus of this research is on one of these spans, Span 2, carrying southbound traffic on four lanes. The steel girders are built-up sections with varying flange thickness and varying girder lengths (~32- 40 m or ~105-131 ft.), resulting in a skewed span.

Throughout the research period measurement sessions have been made at the US202/NJ23 highway overpass to record strain data from the structure under service conditions. More specifically, data from June, September, October, and November 2012 as well as, January, February, March, April, July, and September 2013 has been collected. These data sets provide valuable information about the structural behavior over time.

The neutral axis at three cross-sections (see Figure 1) was studied under dynamic events (when large vehicles pass over the bridge). This probabilistic procedure has been carried out for every measurement session, evaluating the mean and standard deviation; the results are shown in Figure 4. This cross-section shows healthy behavior, the neutral axis does not vary significantly over time and the mean is close to the theoretically expected value.

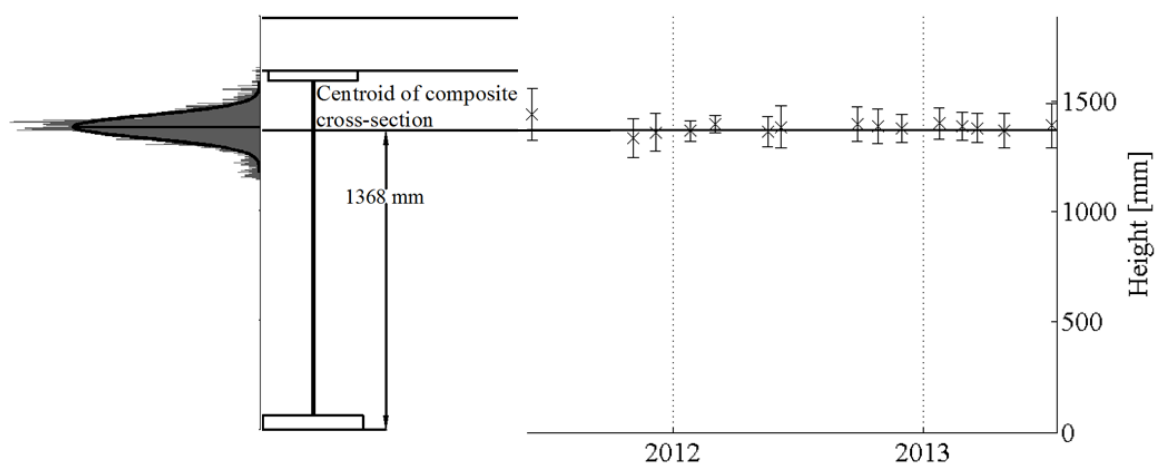


Figure 4. Long-term monitoring of the neutral axis location. The mean for each measurement session along with one standard deviation. This cross-section shows healthy behavior with the mean close to the theoretical location of the neutral axis.

A numerical model of span 2 of the US202/NJ23 was created in order to verify that the variation of the location of the neutral axis is a consequence of the dynamic event. The model was created in the analysis software ABAQUS, see Figure 5 (Dassault Systemes 2011). The model is built with S4R shell elements which are 4-node general-purpose shell, reduced integration elements with hourglass control and finite membrane strains (Dassault Systemes 2011). The model was used to study the neutral axis location under dynamic truck loading. A typical truck load was created with a system of six moving point loads, representing a truck with three axels. The magnitude of each force and the distance between forces was based on an AASHTO truck (AASHTO 2012), see Figure 5.

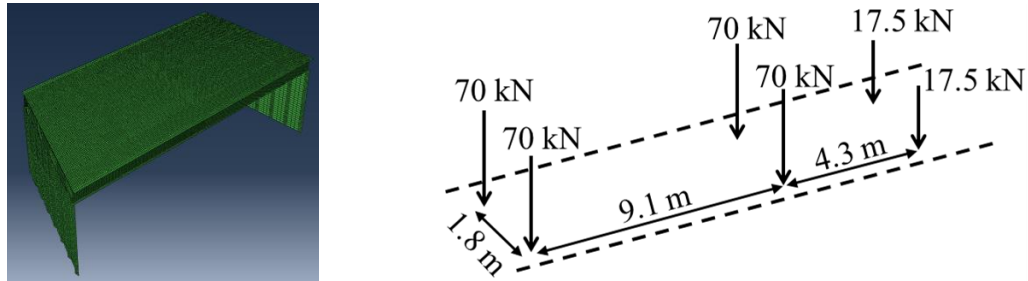


Figure 5. Numerical model of the study span of US202/NJ23 and the simulated load pattern.

Figure 6 shows the strain at locations 5.1, 5.2, and 5.3 during a truck passage as well as the response of the numerical model at the same location during the passage of the simulated load. It is important to note that events observed on the real structure are subject to a large range of uncertainties related to the loading conditions. In particular the load magnitudes are unknown and vary from truck to truck, the location of the load is unknown, i.e. which lane the truck is driving on, and the number of trucks on the bridge at any given time is also uncertain. Since the simulated truck moves on the lane located above Girder 5 and its speed is different from the real load, direct quantitative comparison of strain values is not possible. However, strain responses shown in the figure are qualitatively similar, and this, in general, validates the model. Our assumption is that as long as the structure is in the linear regime the magnitude of the strain is not of importance. However, what does matter is the time dependent characteristic of the event which has been captured well in the simulation.

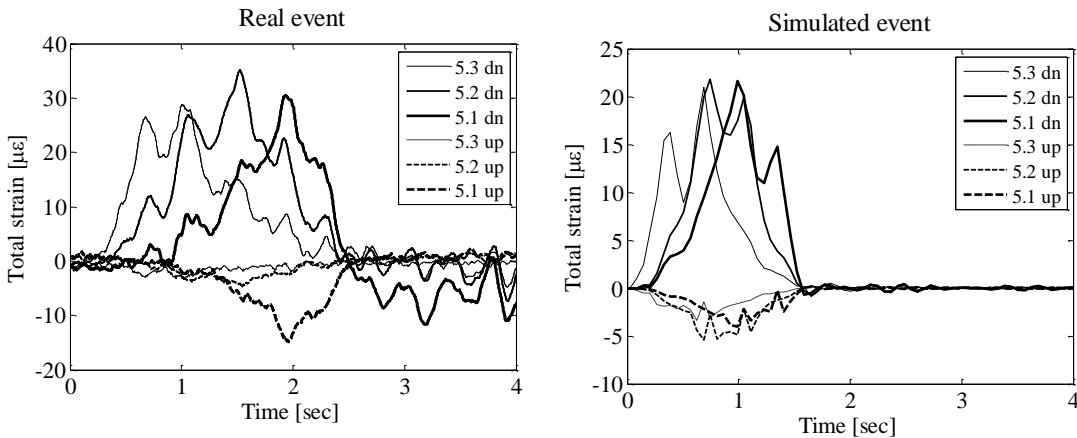


Figure 6. Dynamic event: total strain at location 5.1, 5.2, and 5.3 under the real event and simulated event.

Figures 7a and 7b show the strain diagram at location 5.2 as the result of numerical simulation due to the dead load and during the simulated dynamic event, respectively. Under dead load the neutral axis location is constant, although discontinuities are observed between the concrete slab and the steel girder when the strain magnitudes increase. During the simulated dynamic event the neutral axis is observed to vary over the height of the cross-section. These are important results, as they correlate well with observations made on the real structure, and demonstrate that the neutral axis moves due to dynamic actions.

The location of the neutral axis obtained from the numerical simulation, however, does not coincide with the theoretically obtained values or the observations in the field. This could be mitigated by changing the Young's modulus in the numerical model, but unreasonably high Young's moduli are required to reach the target value and further investigation is needed to fully explain this discrepancy.

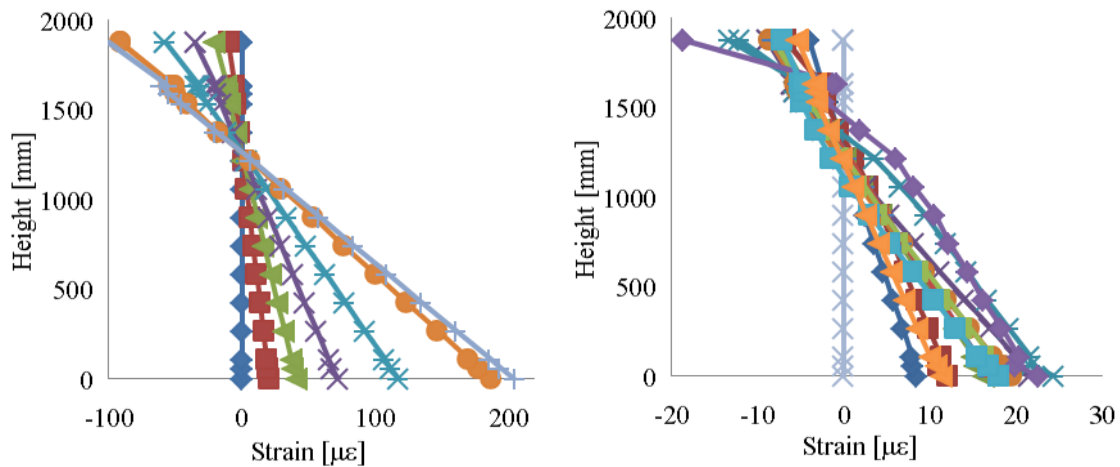


Figure 7. Strain diagram from numerical model. a) Dead load applied to the structure, the neutral axis is constant. b) Dynamic event applied to the structure, the neutral axis varies.

Influence of damage to the position of neutral axis

In order to assess the influence of damage to the position of the neutral axis, a scale model of a bridge with artificially inserted damage was instrumented with a monitoring system. The model was then tested with static and dynamic loads. A monitoring system with 26 sensors was designed and installed, see Figure 8 and 9. Figure 8 shows a cross-section of the structure. Location A has a plastic sheet installed horizontally in the concrete to simulate delamination, location F does not have artificial damage and is considered healthy, and location K has a vertical sheet of plastic installed in the concrete simulating a crack reaching the surface. Four long-gauge fiber-optic strain and temperature sensors were installed in each of these cross-sections (depicted as circles in Figure 8). Additionally thermo-couples (type “K”) were installed in the concrete at location F. A parallel sensor topology was chosen in order to be able to calculate curvature of the cross-section as well as studying the strain distribution through the cross-section. The sensors installed on the steel girders were surface mounted (see Figure 9) similar to the sensors installed on the real structure. The sensors in the concrete provide additional information about the girder-concrete interaction, and this is not available on the real structure. The aim of installing sensors

both on the steel and in the concrete is to be able to provide recommendations on the most effective sensor topology.

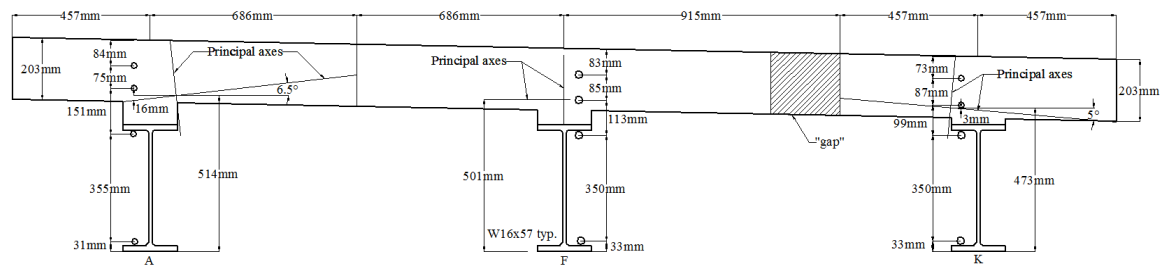


Figure 8. Cross-section of the test structure. Three steel girders supporting a concrete slab. Four strain sensors are installed in three cross-sections. Location A has delamination, location F is healthy, and location K has a crack.

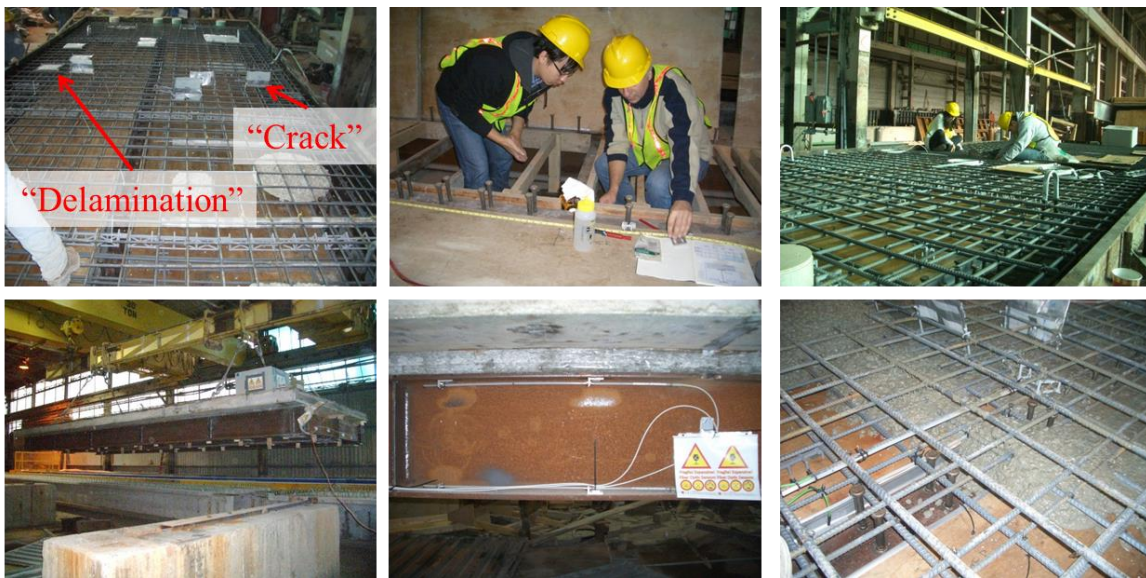


Figure 9. Test structure. The artificial damage is created by placing plastic sheets in the concrete. The sensors are surface mounted on the steel flanges and embedded in the concrete.

Figure 9 shows the rebar cage before pouring of the concrete with labels pointing to the artificially delaminated and cracked locations. It also shows the installation of the steel and concrete sensors as well as the structure after the curing of the concrete. After the sensors were installed and the concrete had reached sufficient strength, the structure was transported to the Rutgers University Livingston Campus. The structure was tested both with static and dynamic loading. Measurements were taken using the fiber-optic sensors. Additionally, LVDT's were installed at the sensor locations A, K, and F during the static testing for comparison with deflection calculations. The dynamic tests were used to calculate the location of the neutral axis. Figure 10 shows the test structure with the test load on it.



Figure 10. Test structure with test load. The photo is taken during static testing.

Four dynamic tests were conducted as follows. The truck was backed up on to the structure and then driven off as quickly as possible in an effort to create a similar load as the real structure experiences under traffic loading. The data set was studied in three different ways using the concrete sensors, the steel sensors, and all four sensors. This is illustrated in Figure 11, where the strain diagram on the left shows how by analyzing different groups of sensors results in different conclusions regarding location of neutral axis (and structural behavior in general). In particular, for the example shown in the figure, analysis of the concrete sensors only might lead to the conclusions that the neutral axis is high, and analysis of the steel sensors only might lead to the conclusion that the neutral axis is low. However, the analysis of all sensors (by finding the best fit through all the points) might lead to the conclusion that the neutral axis is located at the centroid. Understanding which combination gives the most accurate conclusion is crucial for accurate assessment of the data. The histograms to the right of the figure are obtained from the healthy location (F), during the four dynamic tests and the results are summarized in Table 1, along with the results from the other two (damaged) locations (delaminated A and cracked K). Figures 12 and 13 show the histograms from the steel sensors for damaged locations A and K.

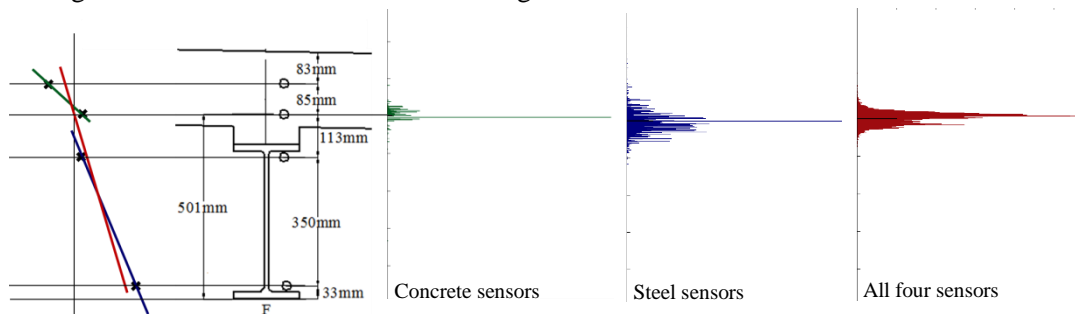


Figure 11. Recorded dataset from concrete and steel sensors separately, and from all four sensors together. On the left, a potential scenario is illustrated where studying different combination leads to different conclusions. On the right the histograms for the healthy location.

Table 1. Summary of the results from dynamic testing for the three locations, A, F, and K using the three different sensor groups: in concrete, on steel, and all four sensors.

[mm]	A (delamination)			F (healthy)			K (cracked)		
Theoretical	514			501			473		
	Concrete	Steel	All	Concrete	Steel	All	Concrete	Steel	All
Mean	501	553	535	512	494	503	495	499	489
Standard deviation	638	27	9	471	27	15	41	24	9

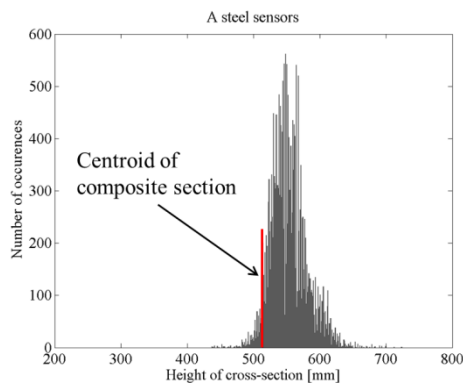


Figure 12. Delamination is created by placing a plastic sheet horizontally in the concrete. Photos show the sheet and the sensor installed next to it. The histogram is from the measurements of the steel mounted sensors from the delaminated cross-section.

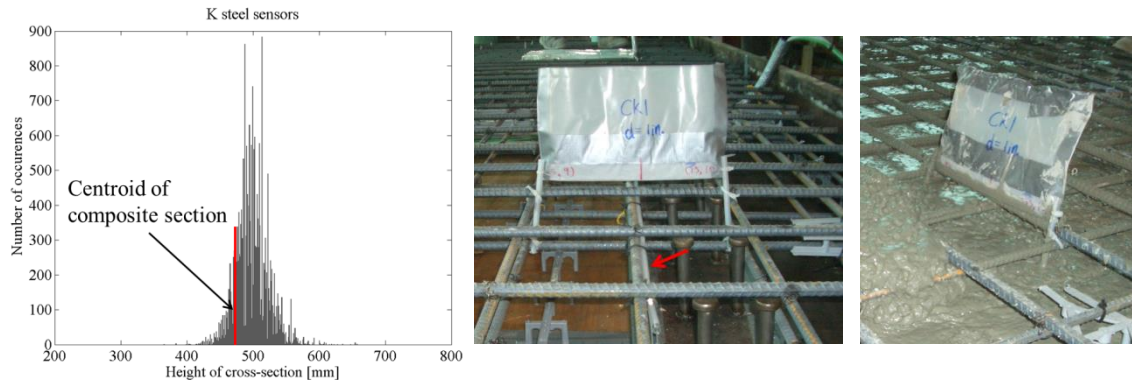


Figure 13. The crack is created by placing a plastic sheet vertically in the concrete. Photos show the sheet and the sensor installed next to it. The histogram is from the measurements of the steel mounted sensors from the cracked cross-section.

The results summarized in Table 1 show that for the healthy cross-section the location of the neutral axis calculated from the measurements practically coincides with the theoretically calculated location of the centroid of stiffness, while at the damaged cross-sections this is not the case. This supports our assumption that the neutral axis in damaged cross-sections changes its location. However, at the damaged cross-sections the neutral axis was assumed to move to lower values, while in the tests it moved to higher values. The reasons for these unusual results are not fully explained and will be addressed in the future research.

Evaluation of deformed shape from strain measurements

Data from the static tests were used to calculate the vertical displacement at the midspan of the scale model using double integration of the curvature. The curvature is calculated as the slope of the lines shown in Figure 11. In addition to the strain sensors three LVDT sensors were installed to measure vertical displacement directly during the static tests. The aim was to assess the accuracy in determination of vertical displacement from the double integration of curvature.

Figure 14 shows the truck and the scale model during the testing. The solid line in the figure represents the curvature diagram due to the truck load according to the linear theory of beams, whereas the dashed line represents the curvature diagram measured by the parallel sensors at the center of the span. Three integration rules were used to evaluate the double integral of the curvature. These are Trapezoidal rule, Rectangular rule I, and Rectangular rule II. The difference between the three rules is illustrated in Figure 14.



Figure 14. Static test. The truck applies two point loads to the structure. The corresponding curvature diagram is shown. The solid line represents the linear theory of beams and the dashed line corresponds to the measured value at midspan. The three integration rules: Trapezoidal, Rectangular I, and Rectangular II are shown below.

The Trapezoidal rule estimates the area as two triangles lying within the dashed lines, Rectangular rule I defines a rectangle that covers half the length of the beam, assuming that the curvature at the end of the beam is zero, and Rectangular rule II defines a rectangle that covers the whole length of the beam. The Trapezoidal rule and Rectangular rule I give the same result in this study, since only one curvature measurement is available along the length of the beam (they would be different if more sensors were installed along the structure). Rectangular rule II was added in this study to compensate for the lack in instrumentation.

The dataset was studied in three ways, using the concrete sensors and steel sensors separately and using all four sensors together. Figure 15 shows the results from location F, with the three different datasets, the three integration rules, and the independent measurements made with the LVDTs. The results confirm that in this case the Trapezoidal rule and Rectangular rule I give the same estimation of the displacement. They underestimate the displacement compared with the LVDT measurements. Rectangular rule II on the other hand overestimates the magnitude of the displacement. The range between the values calculated with the concrete sensors, steel sensors, and all four sensors varies between 0.01-0.07 mm for the Trapezoidal rule and Rectangular rule I and 0.02-0.26 mm for Rectangular rule II.

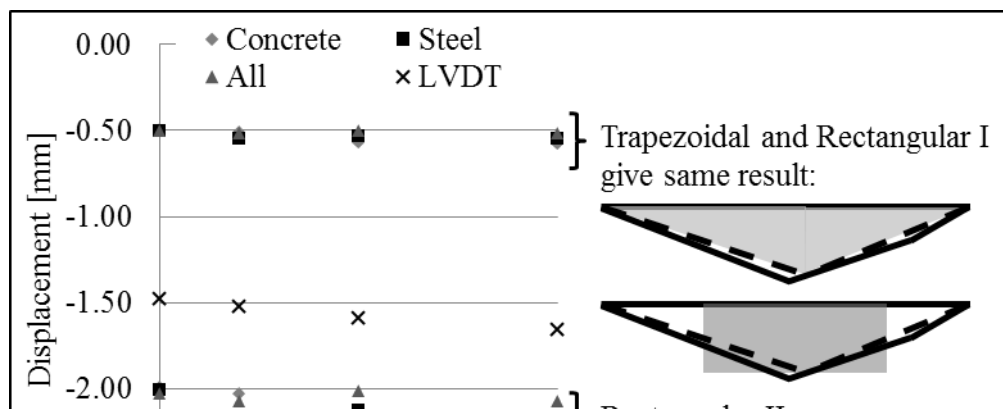


Figure 15. Displacements calculated by double integration using the Trapezoidal rule, Rectangular rule I, and Rectangular rule II for three sensor combinations, concrete, steel, and all. The LVDT measurements lie between the two estimations.

Since the variation between the three datasets (concrete, steel, and all) is relatively small, the measurements from the steel sensors can be used to improve the accuracy in determination of the deformed shape. Steel sensors are chosen to simulate real on-site conditions (i.e., as for US202/NJ23 overpass). The improved solution is based on a linear combination of Trapezoidal and Rectangular II. The coefficients of the linear correlation were found by linear regression based on the least square method.

The results are shown in Figure 16. The displacements were known from independent measurements (LVDT's) and the constants of the linear combination between the integration rules were therefore determined by the least square method. However, the objective was to be able to determine the vertical displacements with the strain measurements alone. In order to achieve that objective it would be necessary to study the properties of the integration rules, the associated errors, and different load scenarios in more detail. In addition, probably the most important factor is true theoretical behavior of structure. Indeed, while the results presented in Figure 16 show the potential of the methodology, the evaluation of the accuracy in determination of deformed shape depends mostly on the correlation between the true and theoretical structural behavior.

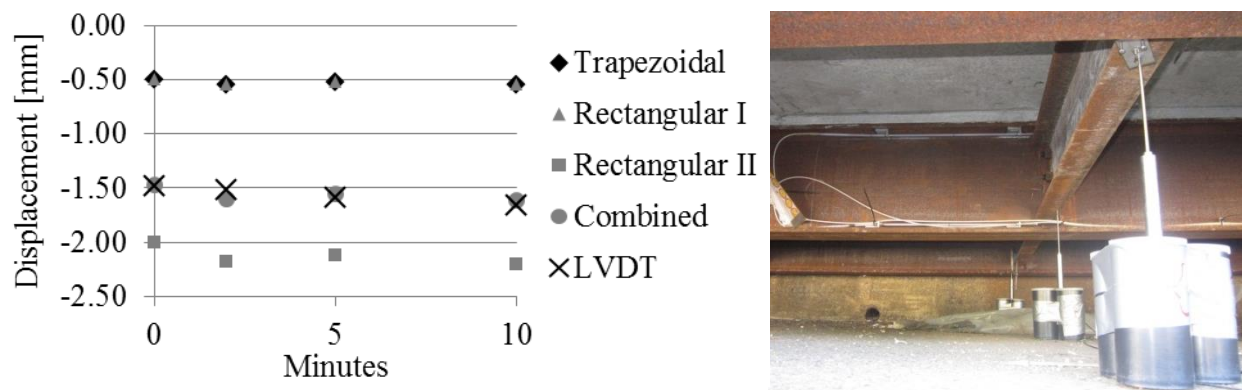


Figure 16. Displacement at midspan, using steel sensors at location F. The results from the three double integration methods are shown, the combination of the Trapezoidal and Rectangular II, as well as the measurements from the LVDTs. The photo shows LVDTs as installed at center span during static testing.

The ratio between the curvature and vertical displacement was used in order to assess the agreement

between the theoretical and true behavior of the scale model. This ratio was chosen so that the Young's modulus and moment of inertia would not affect the comparison. The results are shown in Table 2. The theoretical value is close to the values obtained from the Trapezoidal rule and Rectangular rule I. However, the true ratio obtained by combining the strain sensors (to assess the curvature) and LVDT measurements (to assess the vertical displacement) was different from the theoretical value. This is an important finding, as it demonstrates that in the scale model a simple linear theory of beams is not applicable, probably due to the two-dimensional function of the slab and interaction between the girders. Further research thus is needed in order to estimate the accuracy in determination of vertical displacements based on double integration of curvature.

Table 2. The ratio: curvature/displacement according to beam theory, the LVDT measurements, and the three integration rules.

Theoretical	LVDT	Trapezoidal	Rectangular I	Rectangular II
-0.18	-0.06	-0.19	-0.19	-0.05

CONCLUSIONS

Five major conclusions can be drawn from this project:

1. The neutral axis can be located accurately under in-service dynamic loading. This is achieved by using long-gauge strain sensors installed in a parallel topology and by analyzing the statistics of large datasets.
2. The neutral axis location moves during a dynamic event. This was observed on the US202/NJ23 highway overpass and on the scale-model. The behavior was simulated in ABAQUS which showed that the variation in the location of the neutral axis is a consequence of the dynamic event.
3. The Probability Density Function (PDF) of the location of the neutral axis changes due to damage in the cross-section. This was observed in the datasets from the scale-model testing. The PDFs at the two artificially damaged cross-sections were different from the healthy cross-section. As a consequence, the position of neutral axis is changed in the damaged cross-sections.
4. The double integration method used to evaluate the vertical displacement from curvature measurements does affect the accuracy of the evaluation. Trapezoidal rule underestimates the vertical displacement, while the Rectangular rule overestimates the displacements. The most accurate results are obtained by using a linear combination of the two methods.
5. The most accurate results in determination of the neutral axis and deformed shape in healthy cross-sections are obtained by using four sensors within the monitored cross-section; in damaged cross-section the sensors installed in the concrete should be analyzed separately from those installed on steel, otherwise important errors in judgment can be created; however, the sensor installed on the steel girders provide sufficiently accurate results for both healthy and damaged cross-section. This is an important conclusion as in the real existing structures it is not possible to embed the sensors in the concrete slab.

RECOMMENDATIONS

The following recommendations are proposed:

1. The neutral axis can be used as the damage sensitive feature; however, the uncertainty in determination of the location of the neutral axis makes setting the thresholds challenging.
2. For new structures, it is recommended to install at least three sensors in monitored cross-sections, two on the flanges (upper and lower flange) of the steel girders and at least one sensor embedded in the concrete slab.
3. For existing structures, or for new structures with limited budget allocated for monitoring, two sensors could be used per cross-section; the sensors should be installed on upper and lower flange of the steel girder, and they will provide satisfactory accuracy.
4. One instrumented section within the span of the structure is not sufficient to accurately determine deformed shape of the structure, thus at least three cross-sections should be instrumented; in general, if the cross-sections are equidistant the double integration procedure is simpler.
5. Future work is needed to better understand and evaluate the uncertainties in determination of the position of the neutral axis and deformed shape based on series of parallel long-gauge sensors. The evaluation of uncertainty in determination of the position of the neutral axis and the deformed shape could be performed (a) by exploring analytical expressions for influences causing uncertainties, (b) by comparison with statistically analyzed data from real structures, (c) by comparison with FE simulations, (d) by testing and validation in laboratory on small scale specimen, and (e) by validation on large-scale physical model and real structures.

REFERENCES

- AASHTO. The American Association of State Highway and Transportation Officials. 2012. *AASHTO LRFD Bridge Design Specifications, Customary U.S. Units (6th Edition) with 2012 and 2013 Interim Revisions; and 2012 Errata*. “Section 3: Loads and Load Factors.” [Online]. Available: <http://app.knovel.com/hotlink/toc/id:kpAASHTO32/aashto-lrfd-bridge-design> [Accessed: Sep. 5, 2013].
- Dassault Systemes. 2011. *Abaqus 6.11 Online Documentation*. [Online]. [Accessed: Oct. 8, 2013].
- Minnesota Department of Transportation. 2009. “Economic Impacts of the I-35W Bridge Collapse,” Minnesota Department of Employment and Economic Development. [Online]. Available: <http://www.dot.state.mn.us/i35wbridge/rebuild/municipal-consent/economic-impact.pdf> [Accessed: Sept. 28, 2009].
- National Institute of Standards and Technology. 2009. “Civil Infrastructure: Advanced Sensing Technologies and Advanced Repair Materials for the Infrastructure: Water Systems, Dams, Levees, Bridges, Roads, and Highways.” *National Institute of Standards and Technology, White Paper of Technology Innovation Program (TIP), MD 2089, March 2009*. [Online]. Available: http://www.nist.gov/tip/comp_09/white_papers/ci_wp_031909.pdf [Accessed: Sept. 28, 2009].
- Sigurdardottir, D. & Glisic, B. 2013. “Neutral axis as damage sensitive feature.” *Smart Materials and Structures*, 22(7) 075030 (18 pp).
- U.S. Department of Transportation, Federal Highway Administration. 2007. “2006 Status of the Nation’s Highways, Bridges, and Transit: Conditions and Performance.” *US Department of Transportation, Federal Highway Administration, Federal Transit Administration, Report to Congress, March 14, 2007*. [Online]. Available: <http://www.fhwa.dot.gov/policy/2006cpr/index.htm> [Accessed: Sept. 28, 2009].
- U.S. Department of Transportation, Federal Highway Administration. 2013a. “Deficient Bridges by State and Highway System.” *National Bridge Inventory (NBI)*. [Online]. Available: <http://www.fhwa.dot.gov/bridge/deficient.cfm> [Accessed: Jan. 23, 2013].
- U.S. Department of Transportation, Federal Highway Administration. 2013b. “Structure Type by State.” *National Bridge Inventory (NBI)*. [Online]. Available: <http://www.fhwa.dot.gov/bridge/struct.cfm> [Accessed: Jan. 23, 2013].
- U.S. National Archives and Records Administration. 2004. *Code of federal regulation (CFR)*. Title 23. Bridges, Structures, and Hydraulics. [Online]. Available: <http://www.ecfr.gov/cgi-bin/text-idx?c=ecfr&sid=416ea8c3b7835043f3342c9af47423af&rgn=div5&view=text&node=23:1.0.1.7.28&idno=23#23:1.0.1.7.28.3> [Accessed January 28, 2013].
- U.S. Transportation and Infrastructure Committee. 2007. “Structurally Deficient Bridges in the United States.” *Hearing Before the Committee on Transportation and Infrastructure, House of Representatives, 110 Congress, 1st Session (110–67), Sept. 5, 2007*. [Online]. Available: http://frwebgate.access.gpo.gov/cgi-bin/getdoc.cgi?dbname=110_house_hearings&docid=f:37652.pdf [Accessed: Sept. 28, 2009].